ZIBELINE INTERNATIONAL™ PUBLISHING

ISSN: 2521-5035 (Print)
ISSN: 2521-5043 (Online)
CODEN: ESMACU

Earth Sciences Malaysia (ESMY)

DOI: http://doi.org/10.26480/esmy.02.2023.164.173

RESEARCH ARTICLE

QUANTIFYING RIVERBANK EROSION AND ASSOCIATED LAND COVER CHANGES ACROSS THE COASTAL UPAZILA OF HIZLA, BANGLADESH: AN INTEGRATED APPROACH USING GIS AND MACHINE LEARNING

Mst Laboni[a], Shaikh Ashikur Rahman[b], Sonia Khan Sony[c], Muhammad Risalat Rafiq[a]

[a]Department of Geology and Mining, University of Barishal, Barishal-8254, Bangladesh
[b]Water Science and Engineering, IHE Delft Institute for Water Education, Westvest 7, 2611 AX Delft, Netherlands
[c]Department of Botany, University of Barishal, Barishal-8254, Bangladesh
[*]Corresponding Author Email: mstlaboni.bu@gmail.com

ARTICLE DETAILS

Article History:

Received 03 August 2023
Revised 07 September 2023
Accepted 10 October 2023
Available online 16 October 2023

ABSTRACT

Riverbank migration is a common phenomenon in the floodplains of Bangladesh. The continuous changes in river morphology affect its surrounding land-use patterns which pose threats to the life and property of people living near the rivers. The present study utilized thirty-one (1989-2020) years of satellite data to track the erosion-accretion and its influence on land-use and land-cover (LULC) change of Hizla Upazila using GIS-based Modified Normalized Difference Water Index (MNDWI) and Google Earth Engine (GEE) respectively. Statistical analysis revealed the average erosion rate (5.03 km2) is lower than accretion (5.72 km2), resulting in a net land gain of 24.93 Km2. The spatial distribution of erosional activity suggests that the central and western parts of Hizla Upazila are mostly affected, compared to the eastern part, where new deltas are forming. This phenomenon is attributed to the westward movement of the Lower Meghna River (LMR), making the central and western parts of Hizla more vulnerable. The pattern of land-use change manifests that nearby settlements and vegetation are primarily at risk due to channel migration. A significant decrease in total water area (2.1%) and an increase in bare land area (5.1%) between 1997-2010 indicates substantial deposition. Concurrently, there was a decrease in the total settlement (1.53 km2) and vegetation area (9.8 Km2), indicating natural hazards like floods and high-intensity rainfall. The overall kappa accuracy for LULC is over 85% demonstrating its suitability for forecasting. The outcomes of this study will aid the local community, policymakers, and researchers in mitigating risk and ensuring sustainability.

KEYWORDS

Hizla Upazila; Land-use and land-cover (LULC); Riverbank erosion and accretion; GIS; Google earth engine (GEE); MNWDI

1. INTRODUCTION

Bangladesh is one of the world's largest deltaic plains, with about 405 rivers spreading throughout the country. More than seven percent of its lands are occupied by river systems (Billah, 2018). The huge sediment loads carried by three major rivers, i.e., Ganges, Brahmaputra, and Meghna (GBM), have formed the floodplain of this country (Chen et al., 2005; Goodbred and Kuehl, 2000; Raff et al., 2023). Generally, due to rivers' lateral and vertical mobility, floodplains are subject to seasonal and cyclical changes, which also affect land-use patterns (Hazarika et al., 2015a). A fluvial system's two primary geomorphic processes are river bank erosion and accretion, driven by natural events such as flooding, sedimentation, high energy current and anthropogenic influences such as land use patterns (Lane and Richards, 1997; Surian, 1999).

In addition, the spatiotemporal changes in channel shape also depend on numerous factors, including physical, chemical, and geotechnical properties of bank materials, channel configuration, discharge and sediment load, river stage variation, and vegetation cover (Bartley et al. 2008; Julian and Torres 2006; Simon and Collison 2002). From a broader perspective, bank erosion, and accretion play the most crucial role in the dynamics of the overall fluvial system and influence the morphological changes of a floodplain (Mukherjee et al., 2017). Being a part of natural hazards, bank erosion causes the migration of riparian people and the destruction of hydraulic infrastructure and transportation networks (Islam et al., 2014). On the other hand, accretion reduces sediment transportation capacity and impedes navigation (Bizzi and Lerner 2015). In addition, new alluvial land will be created that can be used for agricultural purposes.

The existing LULC of a region is a cumulative output of the interactions between natural as well as anthropogenic variables and processes (Lambin and Geist 2006). Changes in LULC due to erosion and deposition are obvious phenomena in any floodplain, making it the most endangered ecosystem worldwide (Parveen et al., 2018). When the fertile topsoil is removed due to erosion activities, the land loses its agricultural production capacity and becomes barren. Additionally, periodic land cover change owing to bank erosion leaves negative imprints on people's livelihoods, which over time influences their economic, social, and psychological suffering. Hence, detecting temporal variations in LULC patterns is necessary to understand better the environmental dynamics in response to the morphological changes in the river systems.

It is estimated that about 5% (94 out of 489) of the total floodplain

Quick Response Code	Access this article online	
	Website: www.earthsciencesmalaysia.com	DOI: 10.26480/esmy.02.2023.164.173

Cite The Article: Mst Laboni, Shaikh Ashikur Rahman, Sonia Khan Sony, Muhammad Risalat Rafiq (2023). Quantifying Riverbank Erosion and Associated Land Cover Changes Across The Coastal Upazila Of Hizla, Bangladesh: An Integrated Approach Using Gis And Machine Lea rning. *Earth Sciences Malaysia, 7(2): 164-173.*

Upazilas of Bangladesh are directly affected by extensive bank erosion (Rahman, 2010). The LMR downstream stretch of the GBM river system is highly dynamic and undergoes notable morphological changes. The LMR bisects Hizla upazila in Barishal district. People in this area tend to reside near its banks and engage in intensive agricultural activities due to the floodplain's remarkable fertility and seasonal abundance of water. Thus, this region's socioeconomic and environmental conditions are primarily threatened by bank instability. Regarding socioeconomic vulnerability, Hizla Upazila is the most susceptible coastal region of Bangladesh (Jahan et al., 2017).

Worldwide, numerous studies have been carried out to investigate the influence of bank dynamics on land cover change (Chakraborty and Saha, 2022; Hajra et al., 2017; Hazarika et al. 2015b; Masria et al., 2015; Rahman et al., 2022). In Bangladesh, these studies mainly focused on the Brahmaputra and Padma (Debnath et al., 2023; Alam et al., 2023; Arefin et al., 2021) Rivers, situated in the Northern and Northwestern parts. A few researchers have also addressed the phenomenon in the Meghna estuary along the Bay of Bengal (Islam et al., 2021; Kabir et al., 2020). Nonetheless, little attention has been paid to the lower part of the Meghna River. Though assessed bank dynamics and evaluated the future impact of land use change on the ecosystem across LMR, the impact of bank dynamics on land cover change is yet to be done (Mahmud et al., 2020; Hoque et al., 2020). In our focused area Hizla Upazila, issues regarding the impact of storm surges, water quality appraisal, and the biodiversity of fish species have been addressed (Jahan et al., 2017; Islam et al., 2023; Hossain et al., 2012). However, these investigations must incorporate the effects of riverbank erosion on land use patterns to identify the area's vulnerability and risk levels. Thus, monitoring the spatiotemporal dynamics of riverbanks and their influence on land use changes is essential for ensuring long-term sustainability and economic development in this region.

Remote sensing and Geographic Information System (GIS) technique is broadly used for detecting spatiotemporal changes in river morphology and land use (Hassan et al., 2017; Lovric and Tosic, 2016; Rahman and Tripathi 2013; Lo and Shipman 1990; Michalak 1993; Pijanowski et al., 2002). Remotely sensed satellite imageries like Landsat, sentinel 2, and Moderate Resolution Imaging Spectroradiometer (MODIS) data are frequently used as they have broad area coverage, synoptic perspective, and regular data. Time series analysis is helpful in identifying the rate and pattern of erosion accretion and its influence on land use change. Multi-temporal analysis of an area requires dealing with large amounts of data; a major concerning factor as large data size increases the possibility of inaccuracy and is tough to handle. In this regard, the GEE cloud-based platform is incredibly beneficial, considering the ability to analyse substantial spatial regions using high-performance computing resources without downloading (Ghosh et al., 2014).

Besides, advanced machine learning and deep learning algorithms are becoming increasingly popular because of their improved accuracy and automated real-time categorization processes that enable quick change detection (van Leeuwen et al., 2020; Roy, 2021). To address classification issues, trained supervised learning techniques, namely Artificial Neural Networks, Support Vector Regression, and Random Forest (RF), are mainly adopted. In this study RF classifier is used as it has high processing power for unwanted data. The present study estimates the rate and pattern of erosion and accretion of Hizla Upazila and its impact on land use. In addition to improving floodplain management, this study sheds light on the various riverine risks that locals in this area might encounter as a result of the fluvial dynamics of the LMR.

2. METHODOLOGY

2.1 Study Area

The Hizla Upazila is located in the southern half of Bangladesh between 22°50' and 23°05' north latitudes along with 90°25' and 90°43' east longitudes (Figure 1). This Upazila occupies an area of 515.36 km² with a population of 146077. Most of the part of this region is delta type as the mighty Meghna River flows through it and is crisscrossed by several distributaries. The lower part of the Meghna River is formed by the confluence of the Ganges, Brahmaputra, and Upper Meghna River (known as the GBM river system) and falls into the Bay of Bengal. Six Unions (Harinathpur, Memania, Hizla Gaurabdi, Guabaria, Barajalia, and Dhulkhola) of Hizla Upazila reside on both sides of the Lower Meghna River. Because the high load of sediment carried by the GBM river system makes this region unstable and subject to frequent erosion and accretion, the area is also sensitive to several natural hazards, namely floods, cyclones, storm surges, and land use change. As a result, the economy of this region is greatly hampered. Close monitoring is needed to ensure sustainability in this region, which was the prime reason for selecting the study area.

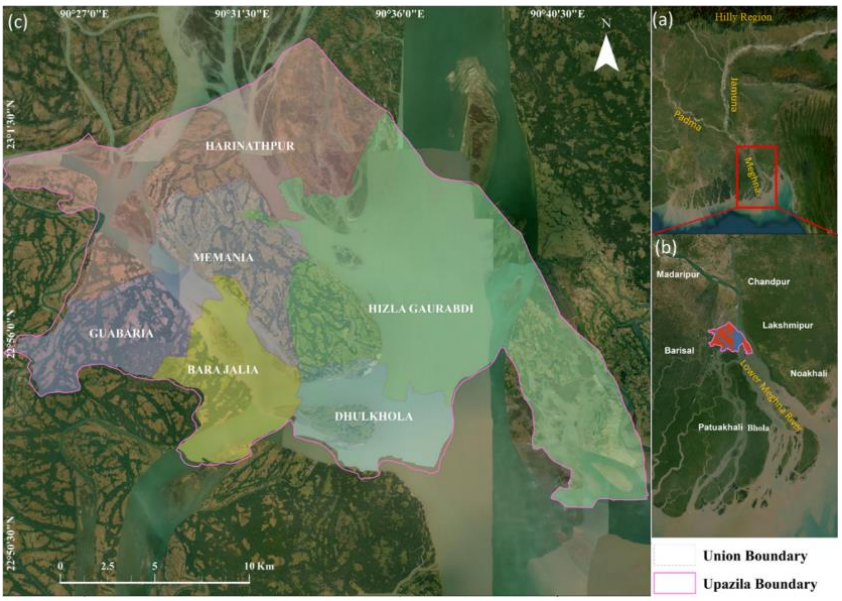

Figure 1: Location of the study area (a) The flow path of three major rivers (Padma, Meghna, and Jamuna) of Bangladesh; (b) Position of Hizla Upazila in relation to the Lower Meghna River (LMR) with surrounding districts; (c) All the unions of this Upazila

2.2 Data Collection and Preprocessing

Six landsat images covering the period ranging from 1989 to 2020 were used in this present study, selected Landsat 5 Thematic Mapper (TM) and Landsat 8 OLI (Operational Land Manager)-TIRS (Thermal Infrared) sensor images based on satellite image quality and availability. For erosion and accretion assessment, Cloud-free Landsat imagery (Table 1) was downloaded from Global Visualization (Glovis) of the United States Geological Survey (USGS) in the years 1989, 1997, 2004, 2010, 2015, and 2020. The study area was delineated according to the Local Government Engineering Department (LGED) Upazila boundary map, followed by georeferencing and converting into vector data. However, Landsat TM and OLI data processing was conducted on the GEE platform for land use classification. A loud screening algorithm with <5% cloud cover was applied to ensure cloud-free optimal imagery for each year. The overall methodology of this research is summarized in a flow chart (Figure 2).

2.3 Total Erosion-Accretion Calculation

Several methods can be adopted for extracting water information from remote sensing imagery, like the single-band and multi-band methods, according to the number of bands used. However, the data from a single band may lead to an over or under-estimation due to mixing up with shadow and noise. Among the multi-band methods, the MNDWI is used to

extract water body information more easily, quickly, and accurately than other classification methods (Li et al., 2013). The MNDWI (Xu 2007) for TM and OLI images is calculated as:

MNDWI = (Green – SWIR) / (Green + SWIR)

For Landsat 7 data, MNDWI = (Band 2 – Band 5) / (Band 2 + Band 5)

For Landsat 8 data, MNDWI = (Band 3 – Band 6) / (Band 3 + Band 6)

The Classified image was then converted into vector format, and the erosion and accretion were measured by comparing the vector data from different periods.

2.4 Land-use Classification and Change Detection

The LULC maps of the study area were prepared based on five major land-use classes: water bodies, bare land, vegetation, and settlement, considering our research objectives. Here, the term "water bodies" refers to both major rivers and other permanent bodies of water; "bare land" indicates sandy terrain and barren lands adjacent to rivers; "vegetation" refers to both natural forest and agricultural land; and "settlements" refers to places with built-up features. While preparing the map in GEE, the Random Forest (RF) algorithm was selected as the classifier because it conveys greater processing power for noise and overfitting. Furthermore, RF usually provides higher accuracy even though it handles complex data of large dimensions. It generates multiple decision trees and classifies a dataset based on the prediction modes for all decision trees. Training samples were collected through visual interpretation and field observations for classification purposes. Field data was collected randomly, maintaining at least 500m distance to minimize spatial homogeneity, and the other reference samples were derived from the high-resolution image of the Google Earth map in different years. Annually, 500 training points were used for LULC classification in four classes.

Table 1: Description of the Collected Landsat Imagery with Resolution and Cloud Cover

Sensor Platform	Path/Row	Acquisition Date	Resolution	Spectral bands	Cloud cover	Data source
Landsat-5	137/44	21-02-1989	30m	1-7 (TM)	<5%	https://glovis.usgs.gov/
Landsat-5	137/44	26-01-1997	30m	1-7 (TM)	<5%	https://glovis.usgs.gov/
Landsat-5	137/44	13-11-2004	30m	1-7 (TM)	<5%	https://glovis.usgs.gov/
Landsat-5	137/44	16-12-2010	30m	1-7 (TM)	<5%	https://glovis.usgs.gov/
Landsat-8	137/44	12-11-2015	30m	1-11 (OLI)	<5%	https://glovis.usgs.gov/
Landsat-8	137/44	27-12-2020	30m	1-11 (OLI)	<5%	https://glovis.usgs.gov/

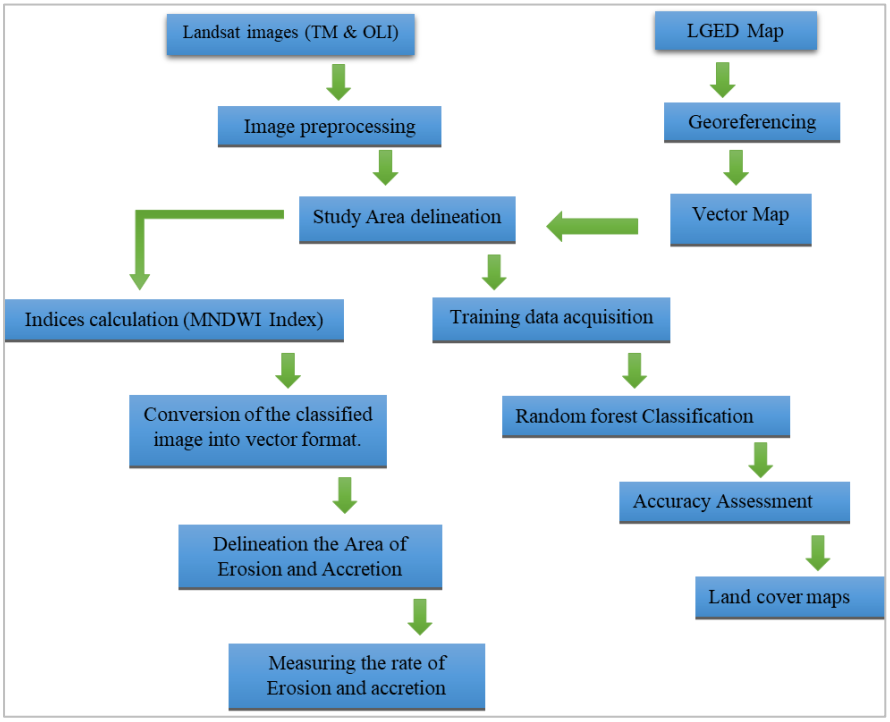

Figure 2: Workflow chart of this research

2.5 Accuracy Assessment

The post-classification accuracy assessment is essential to quantitatively evaluate how well the pixels were sampled into the appropriate land cover classes. The accuracy of the classification algorithm has been evaluated in many recent studies using kappa coefficient (K) based indices, an articulate method of analyzing a single error matrix and comparing the differences between different error matrices. The degree of agreement between classified images and the ground truth is measured using five levels: bad or very poor, fair, good, very good, and excellent, which correspond to values less than 0.4, 0.4 to 0.55, 0.55 to 0.70, 0.70 to 0.85, and greater than 0.85, respectively. In this study, 100 random points were generated for each year in the classified image of the study area, and the points were then validated using the hydrological map, topographic map, Google Earth, and Google Map as reference sources.

3. Results

The rate of erosion-accretion and changes of the LULC in the study region are summarized below. To clearly articulate the findings, and differences, this section provides an in-depth, detailed quantitative analysis of the observed changes. It is structured into two distinct sub-sections, each dedicated to a specific verdict and its corresponding visual representation. Firstly, the information related to fluctuations and trends observed in erosional and accretional activity for the past 31 years due to river dynamics. Secondly, the information related to changing, converting, and validating LULC for different study years.

3.1 Erosion-Accretion Pattern

Six satellite images (1989, 1997, 2004, 2010, 2015, and 2020) have been studied to investigate the morphological changes in the Meghna River for the targeted zone employing remote sensing techniques. Figure 3 illustrates the overall scenario and span of erosion and accretion in Hizla Upazila. Table 2 shows the summarized statistics where the average erosion and accretion rate was 5.03 km^2 and 5.72 km^2 over the period. The accretion rate of this region was even higher from 2004 to 2010, measured at 8.64 km^2 per year. During this period, the north-eastern and south-

eastern bars expanded significantly, forming 27.84 km² of land suitable for settlement and agriculture. In addition, a gain of 10.74 km² was observed between 2015 and 2020, meanwhile, the newly created land in previous years became stable. Contrarily, the years 1997 to 2004 saw substantial erosion, especially in the central region of Hizla Upazila, which comprises Harinathpur, Hizla Gaurabdi, and Memanina Union. The highest reported land loss from erosion occurred during this event (Figure 4), totaling about 8.73 km², and it coincided with the total submergence of a newly formed bar in the Eastern part. Another noteworthy period of erosion occurred from 2010 to 2015 inducing a land loss of 6.87 km², predominately damaging the eastern portion of Hizla Gaurabdi Union. A high degree of instability, mainly driven by the Lower Meghna River, is apparent in the studied area's erosion-accretion pattern (Figure 4). These fluctuations can be attributed to natural factors such as water discharge, velocity, sediment volume, and climatic variations. Over the 31-year study period, total river bank erosion was found to be less than the total amount of accretion, resulting in a net gain of approximately 24.93 km² of land (Table 2).

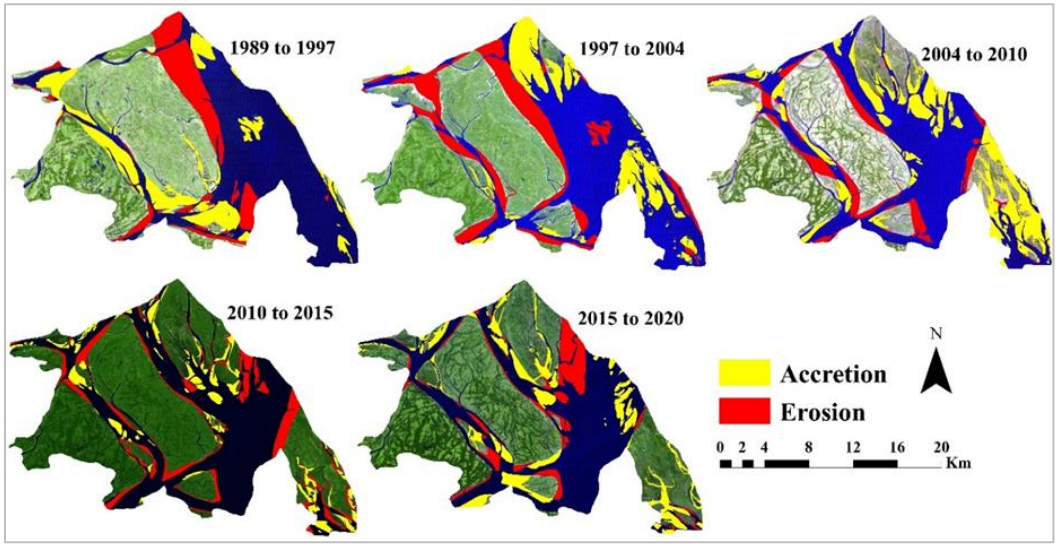

Figure 3: Spatial distribution and pattern of erosion and accretion for a timeline of 1989 to 2020

Table 2: Total area (km²) and rate of erosion-accretion between 1989 to 2020

Year	Erosion Km²	Erosion Rate Km²/year	Accretion Km²	Accretion Rate Km²/year	Gain/loss Km²
1989-1997	37.83	4.72	39.79	4.97	1.95
1997-2004	49.22	6.15	40.48	5.06	-8.73
2004-2010	24.03	4.00	51.88	8.64	27.84
2010-2015	27.41	5.48	20.53	4.10	-6.87
2015-2020	24.03	4.80	34.78	5.79	10.74

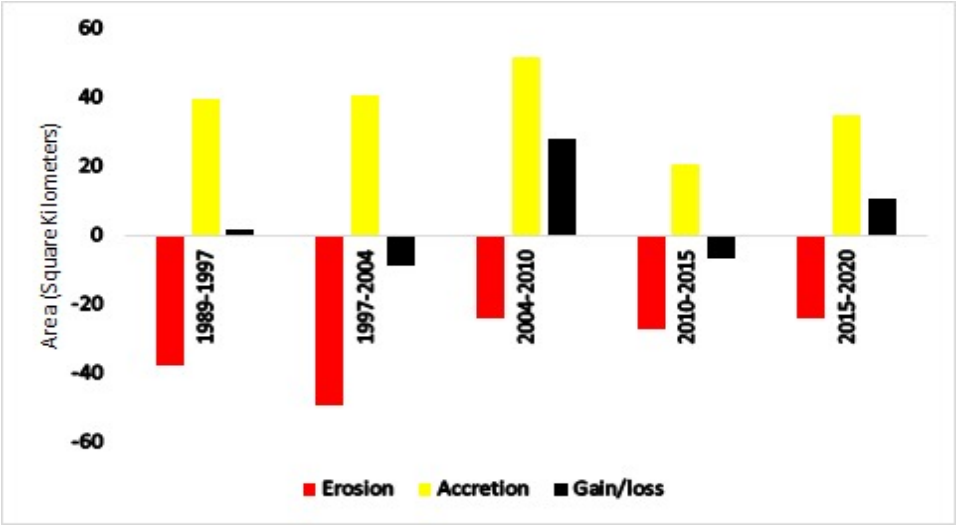

Figure 4: The bar chart represents total riverbank erosion and accretion with resultant gain/loss in different time periods ranging from 1989 to 2020

3.2 Land-Use and Land-Cover Change

Regarding land use classes, the target area is divided into water bodies, settlements, vegetation, and bare land. Land use is a dynamic phenomenon that changes due to the geo-natural process, variation in cropping patterns, seasonal changes, etc. The change in land use pattern is illustrated in Figure 5, and Table 3 contains the quantitative analysis of all the classes. Over the past 31 years, bare land areas have expanded by about 20.31 km² at an average rate of 0.66 km²/year, while waterbodies have declined by 19.1 km² at a mean annual rate of 0.61 km² (Figure 6). This change can be attributed to the deposition of a vast sediment load originating from upstream sources and contributed to the formation of new land, mainly in the eastern part. In another view, it is evident that the extent of bare land has increased by approximately 53.13% from 1989 to 2020 (Table 3); however, the corresponding growth in vegetation cover was only around 0.78%.

The significant erosion and subsequent accretion processes occurring in this area (Figure 4) account for this disparity. A major portion of land consisting of vegetational cover and settlements was eroded from the central and western parts of the study area (Figure 3). Therefore, people residing in these areas were forced to relocate. As the newly formed land

in the eastern part settled, people began to inhabit the area and engage in agricultural activities (Figure 5). The net change is relatively small (0.02 km²), as the total gain and subsidence loss area are roughly equivalent (Table 3). Similarly, vegetation cover is the prominent land type and experienced a negligible net change, losing 1.19 square km. This approach highlights how the river's dynamic nature affects land-use change.

3.3 Validation of Classified LULC

Classified images should also be checked for accuracy before input to an application. The performance of the LULC model concerning a given category or class can be evaluated by considering individual accuracy assessment parameters, and in this study confusion matrix was utilized. The results of the accuracy assessment, including the Kappa coefficient, User accuracy, and Producer accuracy are displayed in Table 4. The classified images displayed a kappa coefficient of 86%, 93%, 89%, 89%, 87%, and 90% in 1989, 1997, 2004, 2010, 2015, and 2020. Across all those years, the Kappa values exceeded the threshold of 0.85, demonstrating strong agreement between the observed and reference land cover classifications. User accuracy, or the percentage of correctly identified pixels according to the user's assessment, ranged from 96% to 100% for water, 92% to 96% for vegetation, 80% to 88% for settlement, and 84% to 100% for bare land. Moreover, the measurement of how many reference pixels were identified correctly by the classification process denoted as producer accuracy was between 89% to 100% for water, 86% to 96% for vegetation, 81% to 89% for bare land, and 100% for settlements. These findings exhibit the land cover classes' reliability and the methodology's strength and dependability, confirming the data's appropriateness for further research and decision-making.

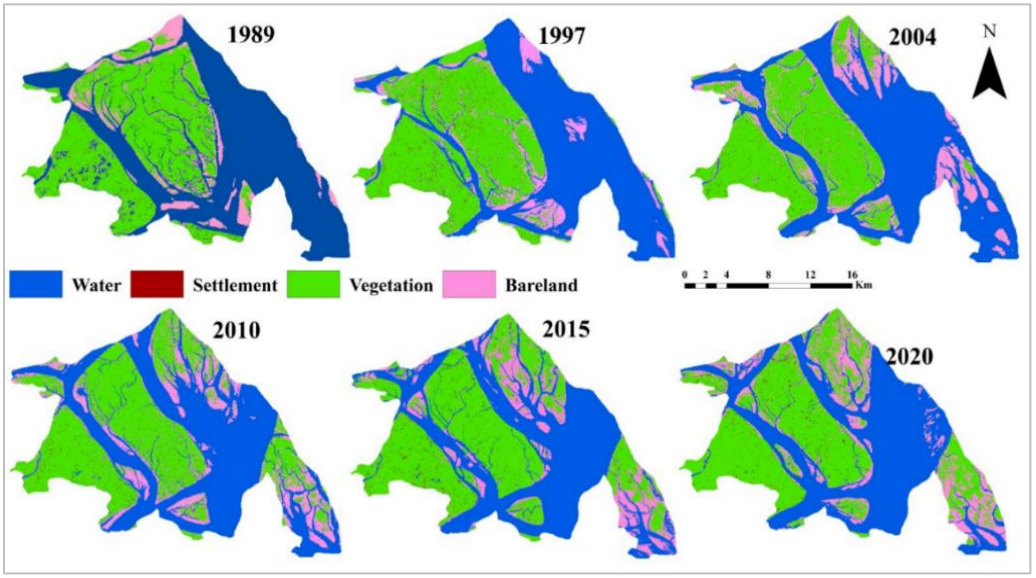

Figure 5: Land use pattern of the study area for the years 1989, 1997, 2004, 2010, 2015, and 2020 calculated using Random Forest (RF) classifier for TM and OLI Landsat imagery in Google Earth Engine (GEE)

Table 3: Statistics of Land Use Classes; Total Area (Km²) and Percentage of Land Acquired by Each Type with Net Gain/Loss Over The 31 Years, 1989 to 2020

Landuse Types	1989		1997		2004		2010		2015		2020		Net gain/loss	
	Km²	(%)	Km²	(%)	Km²	(%)	Km²	(%)	Km²	(%)	Km²	(%)	Km²	(%)
Water	178.89	48.24	173.19	46.70	175.66	47.37	165.42	44.61	158.43	42.73	159.78	43.09	-19.11	-10.68
Vegetation	151.28	40.79	156.44	42.19	138.94	37.47	146.67	39.55	159.16	42.92	150.09	40.48	-1.19	-0.79
Settlement	2.44	0.66	3.31	0.89	1.75	0.47	1.78	0.48	2.80	0.73	2.42	0.65	-0.02	-0.82
Bare land	38.22	10.31	37.89	10.22	54.48	14.69	56.96	15.36	50.53	13.62	58.54	15.78	20.32	53.17
Total	370.83	100.00	370.83	100.00	370.83	100.00	370.83	100.00	370.92	100.00	370.83	100.00	0.00	40.88

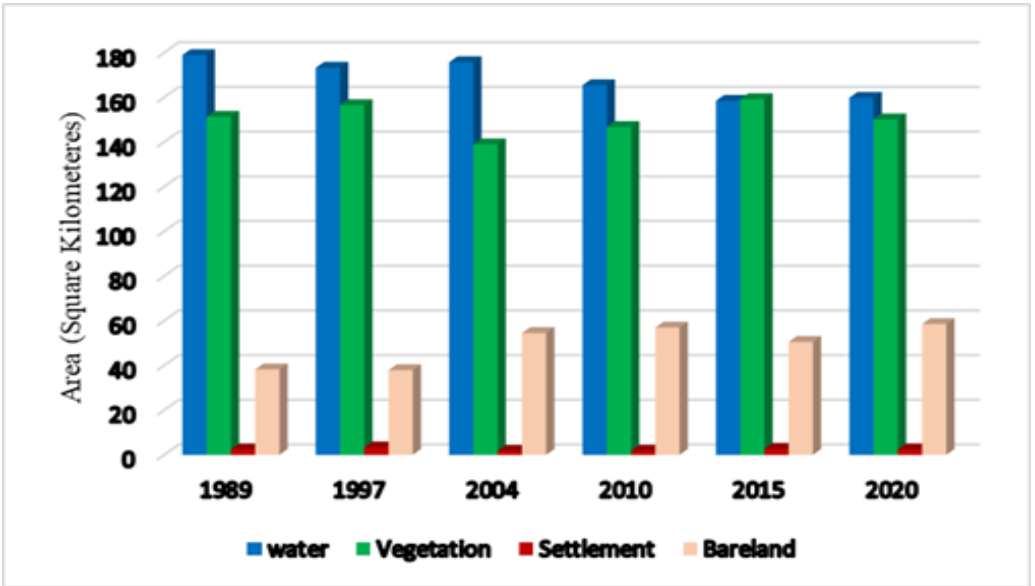

Figure 6: Bar Chart compares the total area (Km2) acquired by four major land types (Water, Vegetation, Settlement, Bareland) represented in different colors accordingly for six individual years (1989, 1997, 2004, 2010, 2015, and 2020)

Table 4: Overall Accuracy of The Land Use Classes Using Confusion Matrix and Kappa Coefficient

2020		Water	Settlements	Vegetation	Bare land	Total	User Accuracy
	Water	30	0	0	0	30	1
	Settlements	0	22	2	1	25	0.88
	Vegetation	0	0	24	1	25	0.96
	Bare land	2	0	1	17	20	0.85
	Total	32	22	27	19	100	0
	Producer Accuracy	0.94	1	0.89	0.89	0	0.93
	Kappa: 0.905						
2015		Water	Settlements	Vegetation	Bare land	Total	User Accuracy
	Water	25	0	0	0	25	1
	Settlements	0	20	3	2	25	0.8
	Vegetation	0	0	24	1	25	0.96
	Bare land	3	0	1	21	25	0.84
	Total	28	20	28	24	100	0
	Producer Accuracy	0.89	1	0.86	0.88	0	0.90
	Kappa: 0.867						
2010		Water	Settlements	Vegetation	Bare land	Total	User Accuracy
	Water	24	0	0	1	25	0.961538
	Settlements	0	21	1	3	25	0.84
	Vegetation	1	0	24	0	25	0.96
	Bare land	1	0	1	23	25	0.92
	Total	26	21	26	27	100	0
	Producer Accuracy	0.93	1	0.92	0.85	0	0.92
	Kappa: 0.894						
2004		Water	Settlements	Vegetation	Bare land	Total	User Accuracy
	Water	24	0	0	1	25	0.96
	Settlements	0	22	2	1	25	0.88
	Vegetation	0	0	23	2	25	0.92
	Bare land	1	0	1	23	25	0.92
	Total	25	22	26	27	100	0
	Producer Accuracy	0.96	1	0.88	0.85	0	0.92
	Kappa: 0.893						
1997		Water	Settlements	Vegetation	Bare land	Total	User Accuracy
	Water	25	0	0	0	25	1
	Settlements	0	21	1	3	25	0.84
	Vegetation	0	0	24	1	25	0.96
	Bare land	0	0	0	25	25	1
	Total	25	21	25	29	100	0
	Producer Accuracy	1	1	0.96	0.86	0	0.95
	Kappa: 0.933						
1989		Water	Settlements	Vegetation	Bare land	Total	User Accuracy
	Water	25	0	0	0	25	1
	Settlements	0	20	2	3	25	0.8
	Vegetation	0	0	23	2	25	0.92
	Bare land	2	0	1	22	25	0.88
	Total	27	20	26	27	100	0
	Producer Accuracy	0.93	1	0.88	0.81	0	0.90
	Kappa: 0.866						

3.4 The Conversion of LULC Categories

Based on the post-classification methods, the change matrix was obtained for 1989 to 1997, 1997 to 2004, 2004 to 2010, 2010 to 2015, and 2015 to 2020, with a relative significance of the major LULC conversions shown in Figure 7. This calculation indicated that a significant portion of the vegetated area was acquired by converting mostly the existing bare lands and a minor part of the settlement area. In contrast, a considerable amount of the vegetative area also converted to bare land at a higher rate from 2015 to 2020 than from 1989 to 1997. The expansion of settlement areas has predominantly involved the replacement of vegetative areas and also a smaller proportion of bare land areas. In this model, the land area turning into waterbodies was regarded as land loss as opposed to land gain, conversion of water bodies into any other classes. The results showed a close correspondence between the observed land gain and loss patterns and the calculated erosion accretion along the river bank, though there were a few minor differences that could be attributed to factors like landfills in inland water areas, errors in the LULC mapping, and limitations in the erosion accretion modelling. A noticeable decline in lake-type wetlands was observed from 1989 to 1997 (Figure 5), suggesting that these areas have been converted to human settlements and agricultural activities.

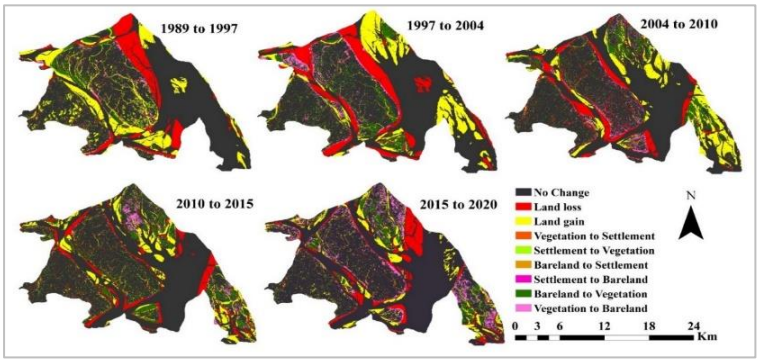

Figure 7: Interchange between major land cover classes in five periods where land converted into waterbodies was considered as erosion, water area converted into any of the classes marked as accretion, and the area remained into same classes is symbolized as no change

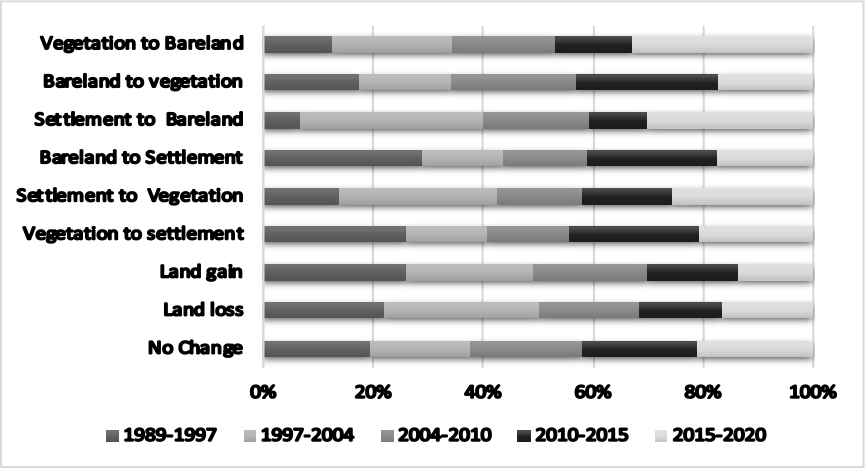

Figure 8: The relative percentage of land type conversion in different periods embodied by the grey color sheds

4. Discussion on Key Findings Based on Previous Literature

Over time, Hizla Upazila has continuously transformed due to the downstream dynamics of the Meghna River, leading to a substantial change in land use and land cover (LULC) within this river floodplain. The shifting and broadening of channels are closely connected to erosion and deposition processes along riverbanks. Throughout the study period, accretion consistently exceeded erosion. A notable occurrence was rapid erosion on the western side and the emergence of new land on the eastern side due to tectonic factors. Settlement and vegetational areas underwent abrupt changes due to catastrophic flooding from heavy rains and the downstream flow of excess river water from the upstream area.

4.1 Influence of Tectonic Activity on Erosion-Accretion Pattern:

The noteworthy shift of additional land formation in the north-eastern and south-eastern regions is a significant change that occurred throughout the entire period from 1989 to 2020 (Figure 5). This process began in 1989, leading to the establishment of two substantial deltas in these areas. The progression is evident on the land use change map (Figure 7-8), illustrating the stabilization of initially formed bare land followed by subsequent vegetation growth. Over time, communities migrated to these two deltas, capitalizing on favorable conditions for settlement and cultivation. In contrast, the central and western parts of the study area experienced erosion over time, causing resident displacement and agricultural land devastation. This phenomenon could be explained by the gradual westward migration of the LMR due to tectonic influences. Previous studies noted that the erosion rate of LMR is higher on the right bank than the left bank, initiating westward river movement (Mahmud et al., 2020).

Elevation profiles across the Meghna floodplain (Figure 9) reveal a slightly higher elevation on the eastern side of LMR than on the western side. This elevation is linked to the active subduction of the Burma Arc, resulting in the formation of a fold belt and significant accretionary prism in the GBM Delta (Small et al., 2009). The fold belt is situated above the underlying shallow-dipping basal megathrust, where the eastern side of the thrust belt is considered upthrown (Steckler et al., 2016). The LMR intersects the fault line, and the upliftment of the eastern side diverted its course westward, rendering the right bank more susceptible to erosion.

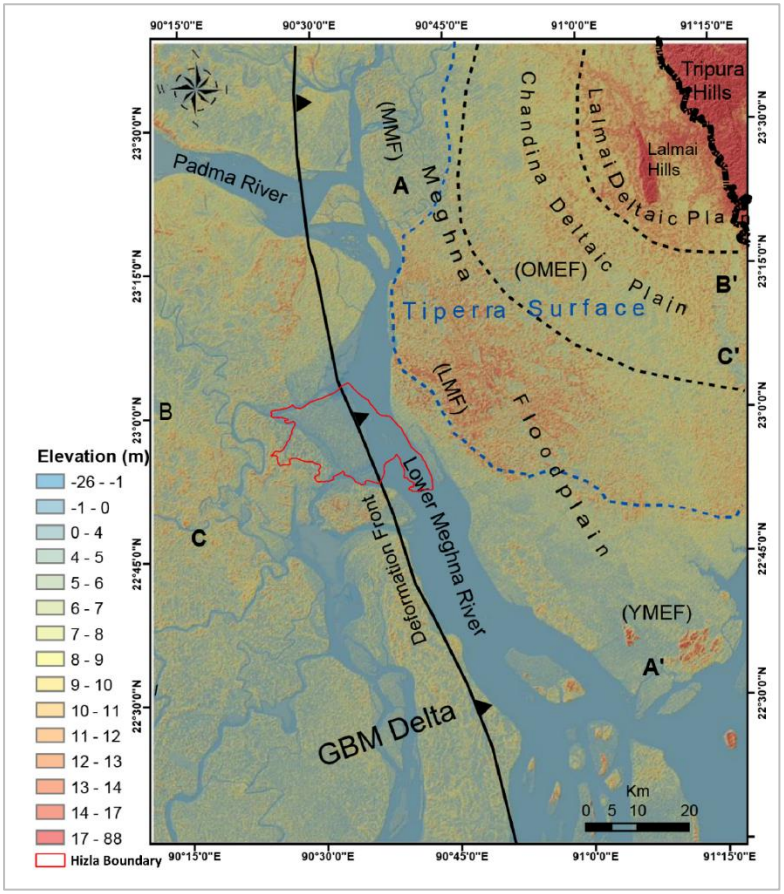

Figure 9: Topography along the bank of Lower Meghna River (LMR) with lithologic boundary after (Rashid, 1991). The tectonic boundary is represented by a heavy black line with tick marks on the upthrown side and the position of Hizla Upazila in red color. Modified after (Mahmud et al., 2020)

4.2 Impact of Extreme Geological Events

On the other hand, the total land area has notably increased over the years, possibly due to sedimentation in this region. An exception is observed between 1997 and 2004 when the land area decreased (Figure 10). Based on climate data, this decrease is assumed to result from rapid erosion caused by floods or high-intensity rainfall during that period. Severe earthquakes in the Himalayan region triggered significant landslides in Nepal, India, and the Kashmir region in 1950, 1963, 1999, 2005, and 2015 (Parkash 2013; Valagussa et al., 2021). A considerable amount of avalanche debris flowed into GBM rivers through various tributaries. Since the fine sediment fraction primarily comprises clay and silt, it moves swiftly through the GBM basin rivers. The deposition of these sediments as they enter low-energy waters tends to alter river morphology.

Furthermore, severe floods occurred in 1998 (68% area of Bangladesh inundated), 2004 (38%), and 2007 (42%) (Hossain et al., 2014). Intense rainfall exceeding averages during monsoons triggers extensive landslides in the upstream region, delivering substantial sediment volumes (Tanvir et al., 2017). The combined impact of earthquakes and floods increased sediment accretion along the confluence and estuary of the Meghna River from 2004 to 2010 and after 2015. This depositional event led to an expansion of bare land area starting in 1997, peaking in 2004 and 2010 (Figure 10). Certain researchers characterized river responses through broadening, enhanced eroding capacity, and migrating sand waves following major depositional events. This explains the dominant role of erosion, contributing to the reduction in bare land area between 2010 and 2020 (Figure 10).

4.3 Factors Contributing Land Cover Change

The GIS-based spatial analysis also revealed patterns of land-type change during the study period. As shown in Figure 10, there is no significant overall change in settlements and vegetation. However, these two land-cover classes displayed the most unstable conditions over the years, and their changes are quite similar. After a sharp decline from 1997 to 2004, both settlement and vegetation areas gradually expanded until 2015. While the settlement area remained stable from 2004 to 2010, vegetational cover increased. Both areas started decreasing at a steady rate after 2015. Natural catastrophes, including cyclones, storm surges, and floods, frequently hit Bangladesh's coastal region, significantly impacting the local population, and often resulting in forced relocations.

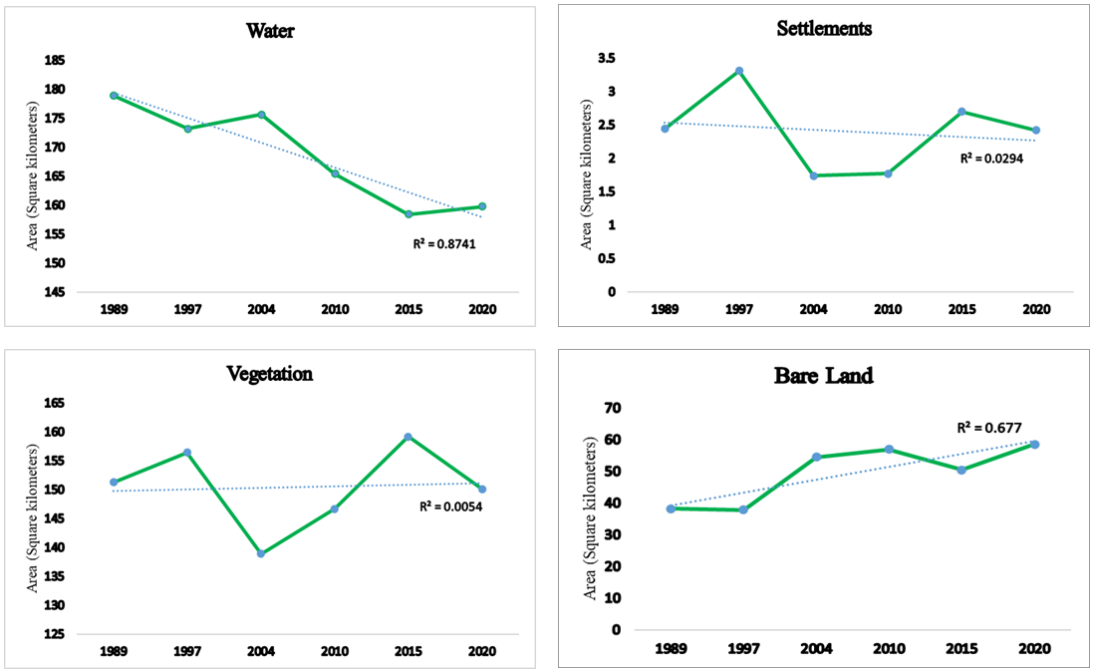

Figure 10: Temporal variation of different land type areas (km^2) from 1989 to 2020

The central coastal region of Bangladesh was severely affected by notable cyclones in May 1997, November 1998, Sidr in November 2007 (Aila, 2009; Agrawala and Van Aalst 2008; Saha, 2015). These cyclones played a vital role in the fluctuation of settlement areas. According to census data, in 1991, the central coastal region had a population of 166,265. By 2004, the population had slightly increased to 174,508, but then declined to 146,077 in 2011. The population size variation aligns consistently with the quantification of settlement areas and shows a similar trend. The powerful cyclones mentioned earlier, along with their effects on the area, and the destruction of agricultural land and loss of livelihood due to frequent flooding, could account for this population decline in this region.

Hizla Upazila is a vulnerable area, and extensive bank dynamics, significantly impacting the socio-economic situation of the region, are believed to be the primary reason for this vulnerability. The newly accreted land (sand char), due to its low fertility and limited use, has poor economic value and falls short in compensating for the loss of native land. Riverbank erosion damages large trees and adversely affects the ecosystem, as it takes years for the char region to develop the necessary soil layers for tree planting. The uncertain nature of farmers' livelihoods, causing wealthier and middle-income farmers to become marginalized or landless, leads to a social crisis. Due to erosion, this area needs more developmental and industrial facilities. Given its erosion-prone nature, population displacement is common as people prefer settling in areas with better access, improved educational and healthcare facilities, career prospects, and enhanced quality of life. Riverbank erosion is one of the most hazardous processes in the study area, with lasting impacts on land use patterns. Thus, this study offers insight into implementing appropriate policies and programs to enhance the livelihood situation in these vulnerable areas.

5. Conclusion

This study comprehensively evaluates spatial and chronological changes in the land area of Hizla Upazila, along with the adaptation of land-use and land-cover (LULC) types to land dynamics. Through detailed analysis of multi-temporal data, we observe that persistent erosion and accretion processes in the lower Meghna River consistently reshape this area, leading to substantial alterations in LULC. Findings reveal a dynamic pattern of land gain and loss across different time frames, with an average accretion rate of 5.72 km^2/year exceeding the average erosion rate of 5.03 km^2/year, resulting in a net land gain. The spatial distribution of erosional activity highlights predominant effects in the central and western parts of Hizla Upazila, while the eastern part witnesses the formation of new deltas over time. This is attributed to the westward movement of the lower Meghna River, rendering the central and western regions more susceptible to erosion. From 2004 to 2010, significant sediment deposition occurred due to extensive landslides upstream triggered by a powerful earthquake. This transported a substantial sediment load downstream. Dominant vegetation cover experienced a decline between 1997 and 2004, potentially due to notable flooding during that period. Conversely, the settlement area reached its minimum extent from 1997 to 2010, indicating that recurrent floods, cyclones, and heavy rainfall may necessitate population relocation. The study's accuracy was verified using User accuracy, Producer accuracy, and Kappa Coefficient. However, it lacks geotechnical analysis to assess land susceptibility to erosion, and it does not account for factors beyond riverbank erosion causing land-use changes. Therefore, additional research is needed before these findings can be applied to policy and planning. Despite its limitations, the study's methodology and analysis provide a basis for future research. Overall, this

study enhances our understanding of how frequent erosion and accretion in the lower Meghna River impact land cover types, laying a foundation for informed decision-making and proactive measures in response to environmental changes in the region.

Authors Contribution

Mst Laboni: Conceptualization, Research design, Data analysis, Visualization and interpretation, Original draft writing, Validation; Shaikh Ashikur Rahman: Data analysis, Visualization and interpretation, Review, and editing; Dr. Sonia Khan Sony: Review and editing; Muhammad Risalat Rafiq: Review and editing.

Acknowledgement

The authors are greatly thankful to Department of geology and Mining, University of Barishal, USGS authorities and Union Parishad Chairman of Hizla Upazila for their cordial help and data availability during this research conduction. Special thanks to Md. Saiful Islam for his support during data analysis.

REFERENCES

Agrawala, S., and Maarten, V.A., 2008. Super Cyclone SIDR 2007: Climate Change Adaptation Mechanisms for Coastal Communities in Bangladesh. Bridge Over Troubled Waters: Linking Climate Change and Development 9789264012769:133–46. doi: 10.1787/9789264012769-7-EN.

Alam, E., and Andrew, E.C., 2010. Cyclone Disaster Vulnerability and Response Experiences in Coastal Bangladesh. Disasters, 34 (4), Pp. 931–54. doi: 10.1111/J.1467-7717.2010.01176.X.

Alam, S., Fuad H., Mohana, D., and Afeefa, R., 2023. Morphology and Land Use Change Analysis of Lower Padma River Floodplain of Bangladesh. Environmental Monitoring and Assessment, 195 (7), Pp. 1–20. doi: 10.1007/S10661-023-11461-W/FIGURES/16.

Arefin, R., Meshram, S.G., and Seker, D.Z., 2021. River Channel Migration and Land-Use/Land-Cover Change for Padma River at Bangladesh: A RS- and GIS-Based Approach. International Journal of Environmental Science and Technology, 18 (10), Pp. 3109–26. doi: 10.1007/S13762-020-03063-7/METRICS.

Bartley, R., Rex, J.K., Aaron, A.H., Peter, B.H., Mark, G.D., and Kinsey-Henderson, A.E., 2008. Bank Erosion and Channel Width Change in a Tropical Catchment. Earth Surface Processes and Landforms, 33 (14), Pp. 2174–2200. doi: 10.1002/ESP.1678.

Billah, M.M., 2018. Mapping and Monitoring Erosion-Accretion in an Alluvial River Using Satellite Imagery - The River Bank Changes of the Padma River in Bangladesh. Quaestiones Geographicae, 37 (3), Pp. 87–95. doi: 10.2478/quageo-2018-0027.

Bizzi, S., and Lerner, D.N., 2015. The Use of Stream Power as an Indicator of Channel Sensitivity to Erosion and Deposition Processes. River Research and Applications, 31 (1), Pp. 16–27. doi: 10.1002/RRA.2717.

Chakraborty, K., and Snehasish, S., 2022. Assessment of Bank Erosion and Its Impact on Land Use and Land Cover Dynamics of Mahananda River Basin (Upper) in the Sub-Himalayan North Bengal, India. SN Applied Sciences, 4 (1), Pp. 1–17. doi: 10.1007/S42452-021-04904-X/FIGURES/13.

Chen, Z., Yoshiki, S., Steven, L.G. 2005. APN Workshop: Ho Chi Minh City. 2005. "Towards Integrated Assessment of the Ganges-Brahmaputra Delta." 268.

Debnath, J., Dhrubajyoti, S., Durlov, L., Nityaranjan, N., Kesar, C., Gowhar, M., Pankaj, K., Suraj, K.S., Shruti, K., and Majid, F., 2023. Assessing the Impacts of Current and Future Changes of the Planforms of River Brahmaputra on Its Land Use-Land Cover. Geoscience Frontiers, 14 (4), Pp. 101557. doi: 10.1016/J.GSF.2023.101557.

Ghosh, A., Richa, S., and Joshi, P.K., 2014. Random Forest Classification of Urban Landscape Using Landsat Archive and Ancillary Data: Combining Seasonal Maps with Decision Level Fusion. Applied Geography, 48, Pp. 31–41. doi: 10.1016/J.APGEOG.2014.01.003.

Goodbred, S.L., and Kuehl, S.A., 2000. The Significance of Large Sediment Supply, Active Tectonism, and Eustasy on Margin Sequence Development: Late Quaternary Stratigraphy and Evolution of the Ganges–Brahmaputra Delta. Sedimentary Geology, 133 (3–4), Pp. 227–48. doi: 10.1016/S0037-0738(00)00041-5.

Hajra, R., Amit, G., and Tuhin, G., 2017. Comparative Assessment of Morphological and Landuse/Landcover Change Pattern of Sagar, Ghoramara, and Mousani Island of Indian Sundarban Delta Through Remote Sensing. Pp. 153–72. doi: 10.1007/978-3-319-46010-9_11.

Hassan, M.A., Suriya, J.R., Masud, H., and Sonia, T., 2017. Remote Sensing and GIS for the Spatio-Temporal Change Analysis of the East and the West River Bank Erosion and Accretion of Jamuna River (1995-2015), Bangladesh. Journal of Geoscience and Environment Protection, 05 (09), Pp. 79–92. doi: 10.4236/gep.2017.59006.

Hazarika, N., Apurba, K.D., and Suranjana, B.B., 2015a. Assessing Land-Use Changes Driven by River Dynamics in Chronically Flood Affected Upper Brahmaputra Plains, India, Using RS-GIS Techniques. Egyptian Journal of Remote Sensing and Space Science, 18 (1), Pp. 107–18. doi: 10.1016/j.ejrs.2015.02.001.

Hazarika, N., Apurba, K.D., and Suranjana, B.B., 2015b. Assessing Land-Use Changes Driven by River Dynamics in Chronically Flood Affected Upper Brahmaputra Plains, India, Using RS-GIS Techniques. The Egyptian Journal of Remote Sensing and Space Science, 18 (1), Pp. 107–18.

Hoque, M.Z., Shenghui, C., Imranul, I., Lilai, X., and Jianxiong, T., 2020. Future Impact of Land Use/Land Cover Changes on Ecosystem Services in the Lower Meghna River Estuary, Bangladesh." Sustainability (Switzerland) 12 (5). doi: 10.3390/su12052112.

Hossain, M., Maruf, M.S., Md, G.U.B., and Saiful, I.B., 2012. Induced Spawning Practices of Different Fishes In The Hatcheries Of Barisal District, Bangladesh. 1 (2).

Hossain, M.S., Md. A.B., and Ripon, K., 2014. Annual Flood Report.

Islam, M.M., Makidul, I.K., Aparna, B., and Most, N.Y., 2023. Physicochemical Variables And Fish Diversity In Hizlamehendiganj Hilsa Sanctuary In Bangladesh. Dhaka University Journal of Biological Sciences, 31 (2), Pp. 289–301. doi: 10.3329/dujbs.v31i2.60887.

Islam, M.S., Md, A.U., and Mallik, A.H., 2021. Assessing the Dynamics of Land Cover and Shoreline Changes of Nijhum Dwip (Island) of Bangladesh Using Remote Sensing and GIS Techniques. Regional Studies in Marine Science, 41, Pp. 101-578. doi: 10.1016/J.RSMA.2020.101578.

Islam, M.S., Sultana, S., and Miah, M.A., 2014. Adaptation of Char Livelihood in Flood and River Erosion Areas through Indigenous Practice: A Study on Bhuapur Riverine Area in Tangail. J. Environ. Sci. and Natural Resources, 7 (1), Pp. 13–19.

Jahan, M., Anisul, H., Rubaiya, K., Mohiuddin, S., and Munsur, R., 2017. Socio-Economic Vulnerability Assessment Due To Storm Surge Hazard In Bangladesh Coast.

Julian, J.P., and Raymond, T., 2006. Hydraulic Erosion of Cohesive Riverbanks. Geomorphology, 76 (1–2), Pp. 193–206. doi: 10.1016/J.GEOMORPH.2005.11.003.

Kabir, M.A., Md, S., Khandaker, T.H., Istiaqe, A.T., Saddam, M.M.H., and Ahmad, A.U., 2020. Assessing the Shoreline Dynamics of Hatiya Island of Meghna Estuary in Bangladesh Using Multiband Satellite Imageries and Hydro-Meteorological Data. Regional Studies in Marine Science, 35, Pp. 101167. doi: 10.1016/J.RSMA.2020.101167.

Lambin, E.F., and Helmut, Geist, eds. 2006. Land-Use and Land-Cover Change. doi: 10.1007/3-540-32202-7.

Lane, S.N., and Keith, S.R., 1997. Earth Surf. Processes Landf. Vol. 22.

Li, W., Zhiqiang, D., Feng, L., Dongbo, Z., Hailei, W., Yuanmiao, G., Bingyu, S., and Xiaoming, Z., 2013. A Comparison of Land Surface Water Mapping Using the Normalized Difference Water Index from TM, ETM+ and ALI. Remote Sensing, 5, Pp. 5530-5549. doi: 10.3390/RS5115530.

Lo, C.P., and Shipman, R.L., 1990. A GIS Approach to Land-Use Change Dynamics Detection. PERS, Photogrammetric Engineering and Remote Sensing, 56 (1), Pp. 1483–91.

Lovric, N., and Radislav, T., 2016. Assessment of Bank Erosion, Accretion and Channel Shifting Using Remote Sensing and GIS: Case Study -

Lower Course of the Bosna River. Quaestiones Geographicae, 35 (1), Pp. 81–92. doi: 10.1515/quageo-2016-0008.

Mahmud, M.I., Mia, A.J., Islam, M.A., Peas, M.H., Farazi, A.H., and Akhter, S.H., 2020. Assessing Bank Dynamics of the Lower Meghna River in Bangladesh: An Integrated GIS-DSAS Approach. Arabian Journal of Geosciences, 13 (14), Pp. 1–19. doi: 10.1007/S12517-020-05514-4/METRICS.

Masria, A., Nadaoka, K., Negm, A., and Iskander, M., 2015. Detection of Shoreline and Land Cover Changes around Rosetta Promontory, Egypt, Based on Remote Sensing Analysis. Land, 4 (1), Pp. 216–30. doi: 10.3390/LAND4010216.

Michalak, W.Z., 1993. GIS in Land Use Change Analysis: Integration of Remotely Sensed Data into GIS. Applied Geography, 13 (1), Pp. 28–44. doi: 10.1016/0143-6228(93)90078-F.

Mukherjee, R., Bilas, R., Biswas, S.S., and Pal, R., 2017. Bank Erosion and Accretion Dynamics Explored by GIS Techniques in Lower Ramganga River, Western Uttar Pradesh, India. Spatial Information Research, 25 (1), Pp. 23–38. doi: 10.1007/S41324-016-0074-2/METRICS.

Parkash, S., 2013. Earthquake Related Landslides in the Indian Himalaya: Experiences from the Past and Implications for the Future. Landslide Science and Practice: Complex Environment, 5, Pp. 327–34. doi: 10.1007/978-3-642-31427-8_42/COVER.

Parveen, S., Jasmeena, B., and Praveen, B., 2018. A Literature Review on Land Use Land Cover Changes. International Journal of Advanced Research, 6, Pp. 1–6. doi: 10.21474/IJAR01/7327.

Pijanowski, B.C., Daniel, G.B., Bradley, A.S., and Manik, G.A., 2002. Using Neural Networks and GIS to Forecast Land Use Changes: A Land Transformation Model. Computers, Environment and Urban Systems, 26 (6), Pp. 553–75. doi: 10.1016/S0198-9715(01)00015-1.

Raff, J.L., Steven, L.G., Jennifer, L.P., Ryan, S.S., John, C.A., Md. S.H., Carol, A.W., Chris, P., Michael, S.S., Dhiman, R.M., Jean-Louis, G., Celine, J.G., Kimberly, G.R., Kazi, M.A., Syed, H.A., Carlson, B.N., Chamberlain, E.L., Dejter, M., Gilligan, J.M., Hale, R.P., Khan, M.R., Muktadir, M.G., Rahman, M.M., and Williams, L.A., 2023. Sediment Delivery to Sustain the Ganges-Brahmaputra Delta under Climate Change and Anthropogenic Impacts. Nature Communications, 14 (1), Pp. 2429. doi: 10.1038/s41467-023-38057-9.

Rahman, C.S., and Nitin, K.T., 2013. Coastal Erosion and Accretion in Pak Phanang, Thailand by GIS Analysis of Maps and Satellite Imagery. Pp. 35.

Rahman, M.R., 2010. Impact of Riverbank Erosion Hazard in the Jamuna Floodplain Areas in Bangladesh. Journal of Science Foundation, 8 (1–2), Pp. 55–65. doi: 10.3329/JSF.V8I1-2.14627.

Rahman, S.A., Islam, M.M., Salman, M.A., and Rafiq, M.R., 2022. Evaluating Bank Erosion and Identifying Possible Anthropogenic Causative Factors of Kirtankhola River in Barishal, Bangladesh: An Integrated GIS and Remote Sensing Approaches. International Journal of Engineering and Geosciences, 7 (2), Pp. 179–90. doi: 10.26833/IJEG.947493.

Rashid, Haroun. 1991. Geography of Bangladesh. Pp. 529.

Roy, B., 2021. Optimum Machine Learning Algorithm Selection for Forecasting Vegetation Indices: MODIS NDVI & EVI. Remote Sensing Applications: Society and Environment, Pp. 23. doi: 10.1016/J.RSASE.2021.100582.

Saha, C.K., 2015. Dynamics of Disaster-Induced Risk in Southwestern Coastal Bangladesh: An Analysis on Tropical Cyclone Aila 2009. Natural Hazards, 75 (1), Pp. 727–54. doi: 10.1007/S11069-014-1343-9/METRICS.

Simon, A., and Andrew, J.C.C., 2002. Quantifying the Mechanical and Hydrologic Effects of Riparian Vegetation on Streambank Stability. Earth Surface Processes and Landforms 27 (5), Pp. 527–46. doi: 10.1002/ESP.325.

Small, C., Michael, S., Leonardo, S., Akhter, S.H., Goodbred, S., Mia, B., and Imam, B., 2009. Spectroscopy of Sediments in the Ganges–Brahmaputra Delta: Spectral Effects of Moisture, Grain Size and Lithology. Remote Sensing of Environment, 113 (2), Pp. 342–61. doi: 10.1016/J.RSE.2008.10.009.

Steckler, M.S., Dhiman, R.M., Akhter, S.H., Seeber, L., Feng, L., Gale, J., Emma, M.H., and Michael, H., 2016. Locked and Loading Megathrust Linked to Active Subduction beneath the Indo-Burman Ranges. Nature Geoscience, 9 (8), Pp. 615–18. doi: 10.1038/ngeo2760.

Surian, N., 1999. Channel Changes Due to River Regulation: The Case of the Piave River, Italy. Earth Surface Processes and Landforms.

Tanvir, H.S.M., Syed, M.A., Wegener, N.M.A., Hassan, S.M.T., and Mamnun, N., 2017. Estimating Erosion and Accretion in the Coast of Ganges-Brahmaputra-Meghna Delta in Bangladesh Himalayan Adaptation, Water and Resilience (HI-AWARE): Research on Glacier and Snowpack Dependent River Basins for Improving Livelihoods (Www.Hi-Aware.Org) View.

Valagussa, A., Frattini, P., Valbuzzi, E., and Crosta, G.B., 2021. Role of Landslides on the Volume Balance of the Nepal 2015 Earthquake Sequence. Scientific Reports, 11 (1), Pp. 1–12. doi: 10.1038/s41598-021-83037-y.

Van, L., Boudewijn, Z.T., and Ferenc, K., 2020. Machine Learning Techniques for Land Use/Land Cover Classification of Medium Resolution Optical Satellite Imagery Focusing on Temporary Inundated Areas. Journal of Environmental Geography, 13 (1–2), Pp. 43–52. doi: 10.2478/JENGEO-2020-0005.

Xu, H., 2007. Modification of Normalised Difference Water Index (NDWI) to Enhance Open Water Features in Remotely Sensed Imagery. Https://Doi.Org/10.1080/01431160600589179 27 (14), Pp. 3025–33. doi: 10.1080/01431160600589179.